

# Strange hadron production in pp, pPb, and PbPb collisions at LHC energies

For the CMS Collaboration

Hong Ni<sup>1,\*</sup>

<sup>1</sup>*Department of Physics and Astronomy, Vanderbilt University, Nashville, TN, United States*

**Abstract.** Identified particle spectra provide an important tool for understanding the particle production mechanism and the dynamical evolution of the medium created in relativistic heavy ion collisions. Studies involving strange and multi-strange hadrons, such as  $K_S^0$ ,  $\Lambda$ , and  $\Xi^-$ , carry additional information since there is no net strangeness content in the initial colliding system. Strangeness enhancement in AA collisions with respect to pp and pA collisions has long been considered as one of the signatures for quark-gluon plasma (QGP) formation. Recent observations of collective effects in high-multiplicity pp and pA collisions raise the question of whether QGP can also be formed in the smaller systems. Systematic studies of strange particle abundance, particle ratios, and nuclear modification factors can shed light on this issue. The CMS experiment has excellent strange-particle reconstruction capabilities over a broad kinematic range, and dedicated high-multiplicity triggers in pp and pPb collisions. The spectra of  $K_S^0$ ,  $\Lambda$ , and  $\Xi^-$  hadrons have been measured in various multiplicity and rapidity regions as a function of  $p_T$  in pp, pPb, and PbPb collisions for several collision energies. The spectral shapes and particle ratios are compared in the different collision systems for events that have the same multiplicity and interpreted in the context of hydrodynamics models.

## 1 Introduction

Recently, the long-range, near-side two-particle correlations in small systems with high-multiplicity [1–4] have brought up an intense debate in the heavy ion field. However, the origin of the observed correlations is still unclear. Among the theories that attempt to interpret these features seen in data, the collective flow scenario of a fluid-like medium provides a natural interpretation [5–7].

In the hydro-dynamic regime, all the particles are supposed to have the same expansion velocity, thus hadrons with different masses will have different  $p_T$  behavior. As the strange quark is the most abundant of the heavier quarks, production of strange particles can be a useful tool to test whether a mass effect is present in these systems. Usually, particle correlations are used to study the flow directly. In the results presented here [8], measurements of strange hadrons ( $K_S^0$ ,  $\Lambda + \bar{\Lambda}$  (hereafter referred to as  $\Lambda$ ), and  $\Xi^- + \Xi^+$  (hereafter referred to as  $\Xi^-$ )) transverse momentum ( $p_T$ ) spectra in three collision systems (pp, pPb, and PbPb) at different center-of-mass energies ( $\sqrt{s_{NN}}$ ) in several different multiplicity ( $N_{trk}^{offline}$ ) and center-of-mass rapidity ( $y_{cm}$ ) regions are presented. With the precise

---

\*e-mail: hong.ni@vanderbilt.edu

measurements of the spectra, particle ratio measurements ( $\Lambda / K_s^0$  and  $\Xi^- / \Lambda$ ) are performed. To explore the possible collective behavior of particles in these systems, a blast-wave model is employed to extract the transverse expansion velocity ( $\beta_T$ ) and kinetic freeze-out temperature ( $T_{kin}$ ) in different multiplicity ranges for each system.

## 2 Results

### 2.1 Invariant mass peaks

The details of event selection and particle reconstruction can be found in [8]. Figure 1 shows some samples of invariant mass peaks. After applying the reconstruction selection criteria, prominent mass peaks are visible, and the background has been largely reduced. To describe the invariant mass peaks, for all the strange particles studied, two Gaussian functions with a common mean are summed up. For the background component, different functional forms are used for different particle species. For  $K_s^0$ , the background is modeled with a quadratic function. For  $\Lambda$ , the analytic form  $Aq^{1/2} + Bq^{3/2}$  with  $q = m - (m_\pi + m_p)$  is used. For  $\Xi^-$ , the form  $Cq^D$  with  $q = m - (m_\Lambda + m_\pi)$  is applied. A, B, C, and D in above analytic expressions are free parameters used in the fitting.

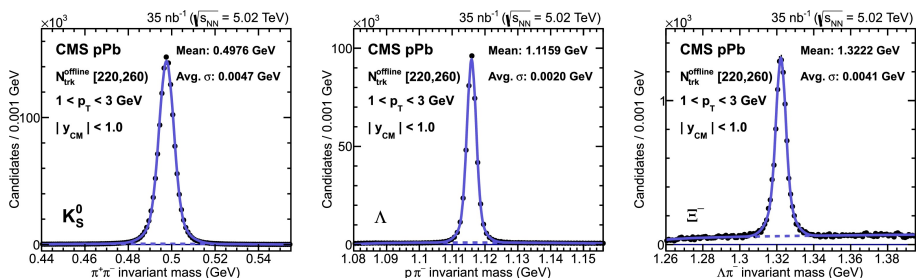


**Figure 1.** Invariant mass distribution of  $K_s^0$  (left),  $\Lambda$  (middle), and  $\Xi^-$  (right) candidates in the  $p_T$  range 1-3 GeV for  $220 \leq N_{trk}^{offline} < 260$  in pPb collisions. Summing up of the charge conjugate states is implied for  $\Lambda$  and  $\Xi^-$ . Figure from [8].

### 2.2 Particle ratios

With the precise measurements of strange particle spectra over different multiplicity ranges, particle ratio measurements can be calculated to check the potential changes of spectra shapes as the multiplicity changes. With the help of a high-multiplicity trigger developed by CMS, particle ratios in similar multiplicity intervals for three different collision systems can be compared. The  $\Lambda / K_s^0$  and  $\Xi^- / \Lambda$  ratios in a center-of-mass rapidity interval  $|y_{CM}| < 1$  are shown in Figure 2. For all multiplicity classes, the  $\Lambda / K_s^0$  ratio increases with  $p_T$  and reaches a maximum at intermediate  $p_T$ , then decreases at higher  $p_T$  while  $\Xi^- / \Lambda$  ratio increases with  $p_T$  and reaches a plateau region at around 3 GeV. For the low  $p_T$  region, in each system, at a given  $p_T$ , the  $\Lambda / K_s^0$  ratio is smaller for higher multiplicity events, and the difference between high and low multiplicity events is larger for smaller systems. No significant difference between high and low multiplicity events is shown for  $\Xi^- / \Lambda$  which can be understood as due to the small mass difference between  $\Xi^-$  and  $\Lambda$  is small.

Among the three collision systems studied, pPb is the only asymmetric system, and a larger radial flow effect is expected on the Pb-going side, as predicted by hydro-dynamic models. With the large

acceptance of the CMS detector, the  $\Lambda / K_S^0$  ratio in different multiplicity intervals on the Pb-going sides and the p-going sides can be compared, and the results are shown in Figure 3. For both low and high multiplicity events, the  $\Lambda / K_S^0$  ratio from the Pb-going direction lies above the results from the p-going direction, with the largest difference observed at high  $p_T$  in high multiplicity events.

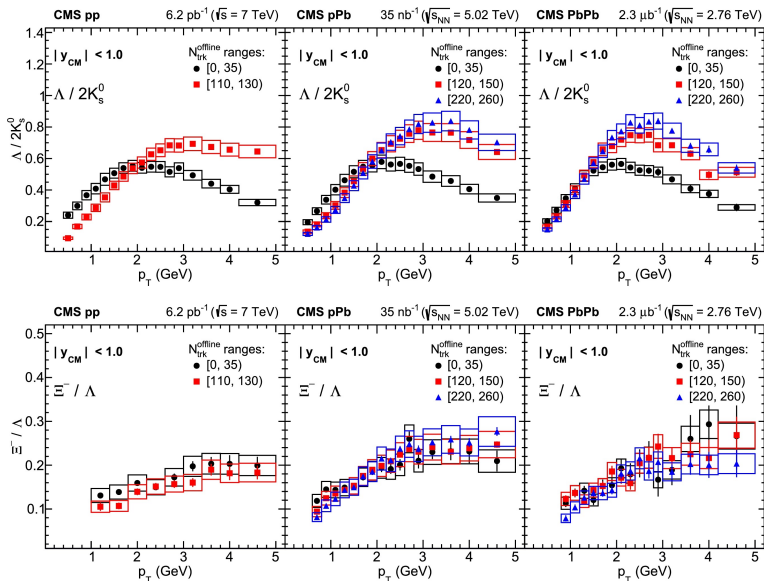


**Figure 2.** Ratios of  $p_T$  spectra for  $\Lambda / K_S^0$  (top) and  $\Xi^- / \Lambda$  (bottom) in the center-of-mass rapidity range  $|y_{cm}| < 1.0$  for pp collisions at  $\sqrt{s} = 7$  TeV (left), pPb collisions at  $\sqrt{s_{NN}} = 5.02$  TeV (middle), and PbPb collisions at  $\sqrt{s_{NN}} = 2.76$  TeV (right). The error bars represent the statistical uncertainties, while the boxes indicate the systematic uncertainties. Figure from [8].

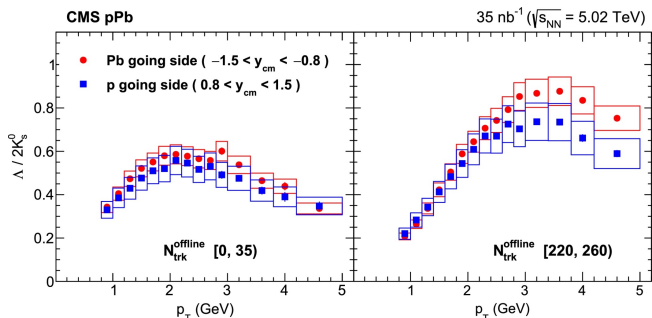


**Figure 3.** Ratios of  $p_T$  spectra for  $\Lambda / K_S^0$  from the  $-1.5 < y_{cm} < -0.8$  (Pb-going) and  $0.8 < y_{cm} < 1.5$  (p-going) rapidity regions in pPb collisions at  $\sqrt{s_{NN}} = 5.02$  TeV (middle). Results are presented for two multiplicity ranges  $0 \leq N_{trk}^{offline} < 35$  (left) and  $220 \leq N_{trk}^{offline} < 260$  (right). The error bars represent the statistical uncertainties, while the boxes indicate the systematic uncertainties. Figure from [8].

### 2.3 Blast-wave fit

Benefitting from the fact that the strange particles are measured down to very low  $p_T$ , the hydrodynamically motivated blast-wave fit [9] can be performed with small uncertainties. In the blast-wave model, common values of  $T_{kin}$  and average radial-flow velocity  $\langle\beta_T\rangle$  are assumed for all particle species. A detailed description of the blast-wave fit can be found in [8]. The extracted values of  $T_{kin}$  and  $\langle\beta_T\rangle$  are shown in Figure 4. According to the plot, for different systems at similar multiplicities the  $T_{kin}$  values are similar, while  $\langle\beta_T\rangle$  is larger for the system with smaller size, which indicates a larger expansion velocity for smaller systems, although the exact meaning of the two parameters is model dependent.

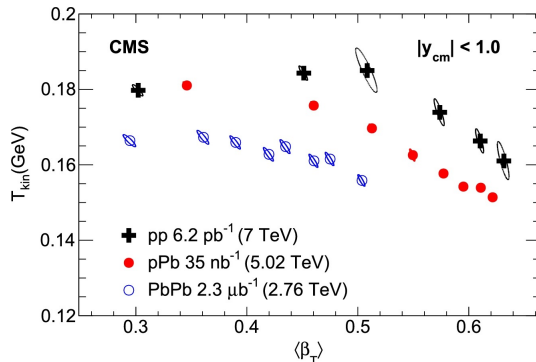


**Figure 4.** The extracted kinetic freeze-out temperature ( $T_{kin}$ ) versus the average radial-flow velocity ( $\beta_T$ ) from a simultaneous blast-wave fit to the  $K_s^0$  and  $\Lambda$   $p_T$  spectra at  $y_{cm} < 1$  for different multiplicity intervals in pp, pPb, and PbPb collisions. The multiplicity intervals are exactly the same as in Figure 2. For the results in this plot, the multiplicity increases from left to right. The correlation ellipses represent the statistical uncertainties. Systematic uncertainties, which are evaluated to be on the order of a few percent, are not shown. Figure from [8].

### 3 Summary

In summary, measurements of strange hadron ( $K_s^0$ ,  $\Lambda + \bar{\Lambda}$ , and  $\Xi^- + \Xi^+$ ) transverse momentum ( $p_T$ ) spectra in three collision systems (pp, pPb, and PbPb) at different center-of-mass energies in several different multiplicity and center-of-mass rapidity regions are presented. With these spectra, particle ratios have been calculated and simultaneous blast-wave fits have been performed. The results are in qualitative agreement with hydro-dynamic models.

### References

- [1] CMS Collaboration, JHEP **09**, 091 (2010)
- [2] CMS Collaboration, Phys. Lett. B **718**, 795 (2013)
- [3] ATLAS Collaboration, Phys. Rev. Lett. **110**, 182302 (2013)
- [4] ALICE Collaboration, Phys. Lett. B **719**, 29 (2013)
- [5] P.Bozek, Phys. Rev. C **85**, 014911 (2012)
- [6] P.Bozek, W.Broniowski, Phys. Lett. B **718** 1557 (2013)
- [7] A.Bzdak, B.Schenke, P.Tribedy, R.Venugopalan, Phys. Rev. C **87** 064906 (2013)
- [8] CMS Collaboration, Phys. Lett. B **768** 103 (2017)
- [9] E.Schnedermann, J.Sollfrank, U.Heinz, Phys. Rev. C **48** 2462 (1993)